2022 7th IEEE International Conference on
Advanced Robotics and Mechatronics
July 9-11, 2022, Guilin, China

2022 International Conference on Advanced Robotics and Mechatronics (ICARM) | 978-1-6654-8306-3/22/$31.00 ©2022 IEEE | DOI: 10.1109/ICARM54641.2022.9959604

A Weight Adaptive Kalman Filter Localization Method Based on UWB and Odometry

Tao Xu[1], Hui Zhang[2], Xidong Zhou[2], Xiaofang Yuan[3], Xuan Tan[3], Jieqingxin Zhang[4] and Hang Zhong[4]

***Abstract*— At present, the indoor positioning methods applied to robots are still subject to many limitations, which restrict the further development of indoor robots. Among the existing localization methods, ultra-wideband (UWB) technology can realize low-cost centimeter-level localization, but the localization accuracy is easily affected by Non-Line-Of-Sight (NLOS). However, using an odometry for position measurement is less susceptible to external environment interference, but it has accumulated errors. In this paper, a Weighted Adaptive Kalman Filter (WAKF) positioning method based on UWB and odometry is proposed, which eliminates the influence of the cumulative error of the odometry on the positioning accuracy to a certain extent, and solves the problem of NLOS positioning error caused by indoor obstacles, to realize the positioning of the robot in complex indoor scenes. The method uses the Kalman Filtering(KF) algorithm to fuse UWB data and odometry data, uses the power difference to identify Line-Of-Sight(LOS) and NLOS scenes, and adaptively adjusts the Kalman filter weights. The method is tested on the Epidemic Prevention and Disinfection Robot (EPADR). The experimental results show that this method meets the demand of indoor positioning, can eliminate the influence of the cumulative error of the odometry and effectively improve the positioning accuracy of the robot in the NLOS scene. Its average positioning error is 0.16m. This method improves the positioning accuracy and robustness of the robot in the indoor environment.**

I. INTRODUCTION

In complex indoor scenes, the positioning of the robot is the basis of its navigation.At present, there are several solutions for indoor positioning. For example, D. Yu et al.[1] used WiFi technology to conduct positioning in complex pedestrian environment. H. Yao et al.[2] realized low-power Bluetooth positioning in indoor scenarios by three-way measurement and least square method. However, both WiFi and Bluetooth have a positioning accuracy of meters. Ali Asghar et al.[3] used RFID technology and linear Kalman filter to achieve indoor cm-level system positioning, but RFID has a small signal range, high power and no communication ability. V. Thio et al.[4] indicated that ultrasonic signals would cause signal loss or reflection in the scene with occlusion, affecting the accuracy of indoor positioning. E. Bernardes et al.[5] carried out indoor positioning of mobile robots based on photodetectors and optical sensors and by using extended Kalman filter and complementary filter. H. Zhang et al.[6] proposed a visual positioning system based on RGB-D camera for building plane scenes to realize real-time positioning of robots. Lidar[7] can achieve centimeter-level positioning, which is suitable for positioning in complex environments, but it has high cost and high power consumption.

Indoor positioning environment is complex and changeable, and its positioning accuracy, cost, power consumption, robustness and so on must be considered comprehensively. Traditional positioning methods are difficult to meet the demand. Ultra-Wideband (UWB) is a wireless carrier communication technology that uses nanosecond non-sinusoidal narrow pulses to transmit data. UWB has many advantages such as strong penetration, low power consumption, good anti-interference effect, low cost, high security, fast transmission rate, and centimeter-level accurate positioning, and it is suitable for indoor positioning. But UWB signals face problems such as NLOS, multipath effects, signal attenuation, and scattering in complex indoor environments, researchers fuse UWB with other technologies. For example, K. Zhao et al.[8] proposed a fusion of RFID and UWB technology to achieve positioning in intelligent warehouse management. K. Wen et al.[9] proposed a positioning method for indoor pedestrians by integrating IMU and UWB with quaternion Kalman filter. X. Zhou et al.[10] proposed an indoor positioning system integrating odometry and UWB. Y. Zheng et al.[11] proposed a comprehensive positioning algorithm for indoor mobile robots based on VO/IMU/UWB. Y. Chen et al.[12] proposed and implemented UWB indoor positioning and tracking system that can effectively alleviate non-line-of-sight scenarios.

In the method of fusion of other technologies, K. Liu et al.[13] proposed a UWB positioning method that can adapt to Kalman filter. S. Zhang et al.[14] proposed an indoor mobile robot autonomous positioning method based on extended Kalman filter integrating wheeled odometry, IMU and UWB. J. Luo et al.[15] controlled mobile robots by fusion of tactile signals and EMG signals.

In view of the above problems and combined with the

This work was supported in part by the National Key RD Program of China under Grant 2021ZD0114503, the Major Research plan of the National Natural Science Foundation of China (Grant No. 92148204), in part by the National Natural Science Foundation of China under Grants 61971071, 62133005, Hunan Science Fund for Distinguished Young Scholars under Grant 2021JJ10025, Hunan key research and development program under Grants 2021GK4011,2022GK2011, Chang sha Science and Technology Major Project under Grant kh2003026, Joint Open Foundation of state Key Laboratory of Robotics under Grant 2021-KF-22-17, China University industry-University-research Innovation Fund under Grant 2020HYA06006.

[1] Tao Xu is with College of Electrical and Information Engineering, Hunan University, Hunan, China (e-mail: xutao1998@hnu.edu.cn)

[2] Hui Zhang is with College of Robotics, also with Robot Visual Perception and Control Technology National Engineering Research Center, Hunan University, Hunan, China (e-mail: zhanghuihby@126.com)

[3] Xiaofang Yuan, [4] Hang Zhong are with College of Electrical and Information Engineering, Hunan University, Hunan, China (e-mail: yuanxiaofang@hnu.edu.cn; zhonghang@hnu.edu.cn)

[2] Xidong Zhou, [3]Xuan Tan, Jieqingxin Zhang[4] are with the College of Electrical and Information Engineering, Changsha University of Science and Tech-nology, Hunan, China (e-mail: xidong-zhou@163.com; tanxuanxf@126.com; 1337503837@qq.com)

978-1-6654-8306-3/22/$31.00 ©2022 IEEE

research status, this paper proposes a Weighted Adaptive Kalman Filter(WAKF) positioning method based on UWB and odometry. The main contributions are as follows:

1. A method is proposed to identify indoor LOS and NLOS scenarios by using the difference between the received power of the UWB anchor and the power of the first path.

2. A WAKF method is proposed to fuse UWB data and odometry data, which eliminates the accumulated error of the odometry to a certain extent and solves the problem of positioning error in indoor NLOS scenarios.

II. UWB POSITIONING MODEL

UWB positioning technology is one of the current popular indoor wireless positioning technologies. The UWB positioning model is based on UWB communication to measure the distance and analyze the coordinates in real time to realize the positioning function. At present, the commonly used ranging methods include Time of Arrival (TOA), Time Difference of Arrival (TDOA), Time of Flight (TOF) and so on. In this paper, the TOF-based ranging method is used for indoor positioning. TOF is a two-way ranging technology. It stamps the time stamp of reception and transmission in the transmitted information [16] and calculates the distance through the TOF of the electromagnetic wave signal between two UWB devices. The distance between two UWB devices can be expressed as the speed of the electromagnetic wave multiplied by the flight time. To achieve two-dimensional coordinate positioning, three anchors and one tag need to be deployed, and three ranging times are performed between each anchor and the tag. A complete positioning requires a total of nine ranging times, as shown in Fig 1.

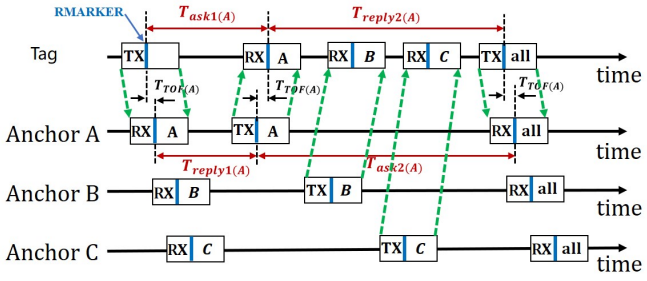

Fig. 1. UWB bilateral two-way ranging

Taking the ranging from Anchor A to the tag as an example, the flight time from Anchor A to the tag is expressed as

$$T_{TOF(A)} = \frac{T_{ask1(A)} \times T_{ask2(A)} - T_{reply1(A)} \times T_{reply2(A)}}{T_{ask1(A)} + T_{ask2(A)} + T_{reply1(A)} + T_{reply2(A)}} \quad (1)$$

The distance from the anchor to the tag is defined as

$$L_i = c \times T_{TOF(i)} \qquad i \in (A,B,C) \quad (2)$$

Among them, $c = 3 \times 10^8 m/s$

The UWB positioning system consists of three anchors and a tag. Assuming that coordinates of the three anchors are known and are $A(x_1,y_1), B(x_2,y_2), C(x_3,y_3)$, the moving tag to be located is $M(x,y)$. L_A, L_B, L_C are the measured distances from the three anchors to the tag, respectively. Draw a circle with the coordinates of the three fixed anchors as the original center and the measured distance from the three anchors to the tag as the radius, and the intersection of the three circles obtained is the area where the tag appears. In this area, the least squares method is used to solve the positioned tag coordinates $M(x,y)$, as shown in Fig 2.

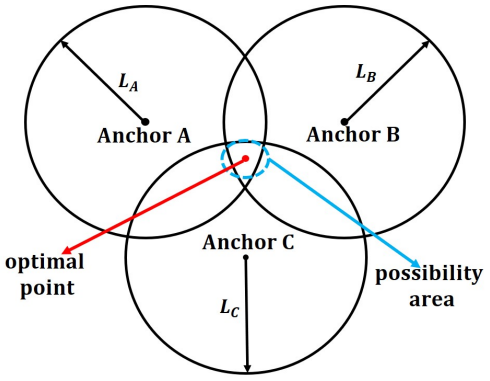

Fig. 2. UWB trilateral positioning

In a two-dimensional plane, the following equation can be obtained from anchor point coordinates, tag coordinates, and the measured distance from anchor point to tag.

$$(x_i - x)^2 + (y_i - y)^2 = L_i \qquad i \in (A,B,C) \quad (3)$$

The coordinates of the three fixed anchor points and their measured distance to the label are known, and the relationship expansion of solving the coordinates of the positioning label can be transformed into a matrix equation and expressed as

$$A \begin{bmatrix} x \\ y \end{bmatrix} = B \quad (4)$$

$$A = \begin{bmatrix} x_2 - x_1 & y_2 - y_1 \\ x_3 - x_1 & y_3 - y_1 \\ x_3 - X_2 & y_3 - y_2 \end{bmatrix} \quad B = \begin{bmatrix} \frac{x_2^2 + y_2^2 - x_1^2 - y_1^2 + L_A^2 - L_B^2}{2} \\ \frac{x_3^2 + y_3^2 - x_1^2 - y_1^2 + L_A^2 - L_C^2}{2} \\ \frac{x_3^2 + y_3^2 - x_2^2 - y_2^2 + L_B^2 - L_C^2}{2} \end{bmatrix} \quad (5)$$

The least squares solution to solve the contradictory equation system as

$$U = \begin{bmatrix} x \\ y \end{bmatrix} = (A^T A)^{-1} A^T B \quad (6)$$

III. UWB AND ODOMETRY FUSION

The positioning accuracy of a system using UWB for indoor positioning is easily affected by factors such as NLOS, multipath effects, and hardware temperature drift. Among them, NLOS has the greatest impact on the positioning accuracy. UWB signals are occluded by obstacles in indoor scenes, causing the signals to reflect or refract and reduce the positioning accuracy. In this regard, we add odometry to UWB positioning for prediction, and use the power difference of UWB anchors to identify NLOS. In

terms of the fusion algorithm of the two sensors, this paper proposes an indoor positioning method to adjusts the weight of KF to adaptively fuse UWB data and odometry data, as shown in Fig 3.

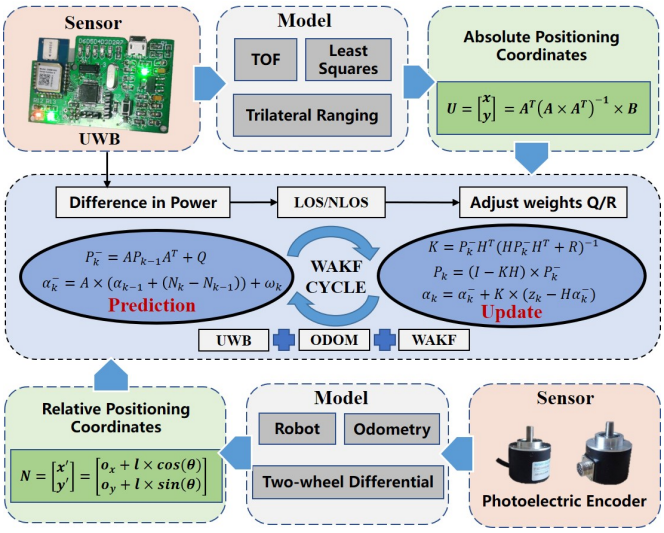

Fig. 3. Fusion of UWB and odometry

A. Odometry Model

The odometry measures the position according to the radian increment of the photoelectric encoder installed on the motor of the mobile robot within a certain period of time. The position measurement of the odometry takes the position at the time of power-on of the robot as the origin of the reference coordinates and accumulates the position and heading of the mobile robot relative to the origin of the coordinates at any time. The odometry is suitable for position measurement within a short distance, and there will be a large degree of measurement deviation with the accumulation of accumulated errors.

Assuming that the wheel diameter of the mobile robot is d, the number of pulses generated by the encoder for one rotation of the wheel is E, and the encoder increment is G. Then the distance coefficient and the distance the robot moves are expressed as

$$\begin{cases} k=\pi d/E \\ l=G\times k \end{cases} \tag{7}$$

The distance between the two wheels of the robot is D and the robotic speed is v. The speed of the left and right wheels can be expressed as

$$\begin{cases} v_{l=}v\pm\omega\times D/2 \\ v_{r=}v\mp\omega\times D/2 \end{cases} \tag{8}$$

Δt is the time interval and θ_0 is the heading angle of the robot at the origin. The angular velocity and heading angle of the robot movement are expressed as

$$\begin{cases} \omega=|v_l-v_r|\times D \\ \theta=\theta_0+\omega\times\Delta t \end{cases} \tag{9}$$

o_x, o_y are the coordinates of the origin and the position coordinates of the robot relative to the origin of the coordinates are decomposed into the x and y directions as

$$N=\begin{bmatrix}x'\\y'\end{bmatrix}=\begin{bmatrix}o_x+l\times cos(\theta)\\o_y+l\times sin(\theta)\end{bmatrix} \tag{10}$$

B. Fusion Process

The traditional Kalman Filter (KF) is a filtering method in which the prediction and correction process is continuously iterated. KF processes the pre-calibrated sensor data to obtain a more accurate continuous range value [17]. The prediction process is to use the state of the previous moment to estimate the state of the current moment, and the correction process is to use the measured value of the current moment. Combined with the estimates, the optimal location for the current state is obtained. The distance measurement of UWB is a discrete control system process, and its measurement error generally obeys the Gaussian distribution. KF has a good filtering effect on the noise of the Gaussian distribution. The KF algorithm is used to input the measurement of the odometry into the system as a prediction process and fuse with the UWB data, so as to correct the measurement error and improve the positioning accuracy. The specific process is as follows.

The observation equation of the system is defined as

$$z_k=H\times U_k+v_k \tag{11}$$

$$H=\begin{bmatrix}1 & 0\\0 & 1\end{bmatrix} \tag{12}$$

Among them, U_k is the coordinates of the UWB positioning mobile tag at time k, and v_k is the measurement noise.

Equation of state is defined as

$$\alpha_k^-=A\times(\alpha_{k-1}+(N_k-N_{k-1}))+\omega_k \tag{13}$$

$$A=\begin{bmatrix}1 & 0\\0 & 1\end{bmatrix} \tag{14}$$

Among them, α_k^- is the a priori estimated coordinate, α_{k-1} is the last filter output coordinate, N_k is the odometry coordinate, and ω_k is the prediction noise.

Estimate the covariance a priori as

$$P_k^-=AP_{k-1}A^T+Q \tag{15}$$

Kalman gain

$$K=P_k^-H^T\left(HP_k^-H^T+R\right)^{-1} \tag{16}$$

The posterior estimation of the corrected data is the output of the KF

$$\alpha_k=\alpha_k^-+K\times(z_k-H\times\alpha_k^-) \tag{17}$$

Posterior estimated covariance

$$P_k=(I-KH)\times P_k^- \tag{18}$$

C. Weight Adaptive Kalman Filter

The positioning of the robot in the indoor scene generally exists in LOS and NLOS. Under NLOS, the UWB signal encounters obstacles and will appear refraction and reflection, resulting in signal attenuation or signal misjudgment. In order to improve the indoor positioning accuracy, it is necessary to eliminate the large error caused by NLOS in the UWB ranging process as much as possible. Q and R in the traditional KF algorithm are used as the weights of the predicted value and the measured value of the filtering model. Different systems need to have corresponding Q and R to match them. If the same value of other states is brought into the system, a large positioning error will occur in the system. Therefore, the UWB positioning system in the case of indoor NLOS needs to dynamically adjust the values of Q and R for adaptive filtering and fusion.

This paper respectively uses the power difference of the received power ($RX_{POWER(i,i\in(A,B,C))}$) of the UWB anchor and the power of its first path ($FR_{POWER(i)}$) to judge the indoor NLOS scene.

$$\begin{cases} RX_{POWER(i)} - FR_{POWER(i)} \le 6 & LOS \\ RX_{POWER(i)} - FR_{POWER(i)} > 6 & NLOS \end{cases} \tag{19}$$

According to experience, the power difference coefficient r has an inverse correlation with Q, and r has a positive correlation with R. In this regard, we introduce the natural constant e to express the relationship between the power difference and the weight.

$$r = \sum_{i=A}^{C} \frac{RX_{POWER(i)} - FR_{POWER(i)}}{3} \tag{20}$$

$$Q = \frac{Q_0}{e^r} \qquad R = R_0 \times e^r \tag{21}$$

Among them, Q_0 and R_0 are the weight coefficients, and the weight coefficient Q_0 of the system noise Q can be set to a small initial value. When the NLOS scene occurs, it means that there will be a large error in the measurement of UWB. At this time, the weight coefficient R_0 of the measurement noise variance R should be set to a larger value, so that the system can trust the prediction from the odometry more and reduce the NLOS brings a large error to UWB positioning, so as to improve the positioning accuracy of the system.

IV. EXPERIMENTS AND ANALYSIS

In order to verify the effect of the indoor positioning scheme of UWB and odometry fusion proposed in this paper, we built a 3 x 2m field for testing in an indoor environment where LOS and NLOS were mixed. The experimental platform uses ERADR. EPADR is mainly composed of four parts: a wheeled mobile chassis based on two-wheel drive, ultraviolet disinfection lamp, disinfectant spray device, and human-computer interaction screen. Its interior is equipped with intel NUC computer and Robot Operating System (ROS). In order to ensure the unnecessary occlusion of the UWB signal in the LOS scene, the UWB positioning tag in this experiment is placed on the top of the robot, and the coordinates of the other three anchors are known, namely: A (0, -2.5), B (0 , 0.5), C(3.5, -1). (Unit: m) The test scene is shown in Fig 4.

Algorithm 1 Weight Adaptive Kalman Filtering Algorithm

Input: UWB measured coordinate U_k, odometry measured coordinate N_k, received power of three anchors $RX_{POWER(i,i\in(A,B,C))}$ and power of the first path ($FR_{POWER(i)}$), weight coefficient $Q_0, R^{'}, R^{''}$

Output: Filter output coordinates α_k

$Differ \leftarrow RX_{POWER(i)} - FR_{POWER(i)}$ //power difference
if $Differ < 6$ **then**
  $R_0 \leftarrow R^{'}$ // $R^{'} < R^{''}$
else if $Differ > 6$ **then**
  $R_0 \leftarrow R^{''}$
else
  $R_0 \leftarrow 0$ //error condition
  $Q_0 \leftarrow 0$
end if
$r \leftarrow \sum_{i=A}^{C} \frac{RX_{POWER(i)} - FR_{POWER(i)}}{3}$
$R \leftarrow R_0 \times e^r$
$Q \leftarrow Q_0 / e^r$
$z_k \leftarrow HU_k + v_k$ //Observation input
$\alpha_k^- \leftarrow A \times (\alpha_{k-1} + (N_k - N_{k-1}))$ //Data Fusion
$P_k^- \leftarrow AP_{k-1}A^T + Q$
$K \leftarrow P_k^- H^T \left(HP_k^- H^T + R\right)^{-1}$
$P_k \leftarrow (I - KH) \times P_k^-$
$\alpha_k \leftarrow \alpha_k^- + K \times \left(z_k - H\alpha_k^-\right)$
return α_k

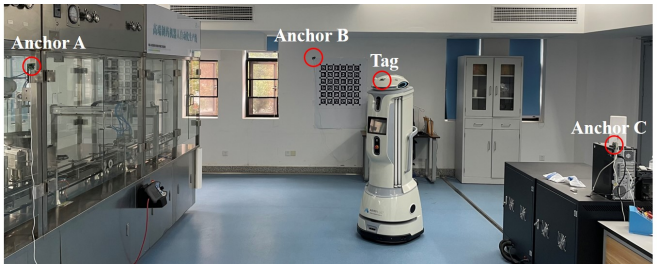

Fig. 4. Testing scenarios

The experiment on the EPADR has three parts. The first part is UWB positioning, the second part is to use odometry for position measurement, and the third part is UWB and odometry fusion positioning.

A. UWB Positioning

When performing UWB positioning, $a, b, c, d, e, f,$ and g on the test site are selected as coordinate measurement points. The movement direction of the robot is e, b, c, f, g, d, a, where $e, f,$ and g are three NLOS scenes generated by human intervention. The robot starts from point a and moves clockwise along the 3 x 2m test field for a circle. When it reaches $e, b, c, f, g, d,$ and a, the robot pauses its movement, and waits for the tester to use a ruler to

measure and record the robot coordinates and then continue to move. The coordinates are recorded as shown in Table I. The maximum error in the case of LOS is 0.27m, and the average error is 0.22m; the maximum error in the case of NLOS is 0.49m, and the average error is 0.46m. Fig 5 shows the distribution of UWB positioning coordinates. It can be seen from Fig 5 that in the NLOS scenario, there is a large error in UWB positioning.

TABLE I
UWB MEASUREMENT DATA

Point	Measuring	Real	Error
e	(1.62,0.48)	(1.70,0.00)	0.49
b	(2.88,0.25)	(3.00,0.00)	0.27
c	(2.85,-2.21)	(3.00,-2.00)	0.26
f	(1.89,-2.45)	(2.00,-2.00)	0.46
g	(0.95,-1.58)	(1.00,-2.00)	0.42
d	(-0.15,-1.96)	(0.00,-2.00)	0.16
a	(0.17,0.09)	(0.00,0.00)	0.19

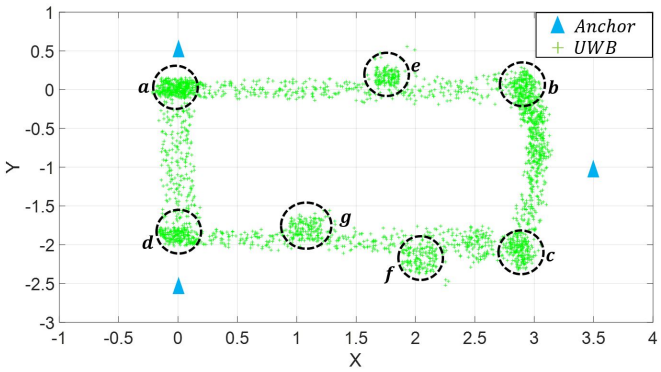

Fig. 5. UWB positioning

B. Odometry Positioning

When using odometry for position measurement, a, b, c, and d on the test site are selected as the coordinate measurement points.The measurement methods is same as the UWB position experiments. The data records are shown in Table II. Fig 6 is the positioning trajectory diagram of the odometry. Fig 6 shows that the positioning of the odometry is closer to the real trajectory of the robot, but there is a cumulative error.

TABLE II
ODOMETRY MEASUREMENT DATA

Point	Measuring	Real	Error
b	(2.97,0.02)	(3.00,0.00)	0.04
c	(2.95,-2.03)	(3.00,-2.00)	0.06
d	(0.09,-1.94)	(0.00,-2.00)	0.11
a	(0.12,0.09)	(0.00,0.00)	0.15

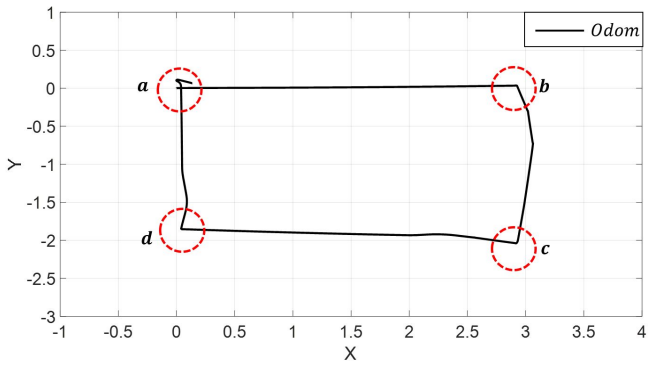

Fig. 6. Odometry measurement

C. UWB and Odometry Fusion Positioning

When performing fusion positioning of UWB and odometry, the motion direction, measurement point, measurement method, and NLOS scene of the robot should be consistent with those of UWB positioning. The experimental data are shown in Table III. In the LOS scenario, the traditional KF method has almost the same effect as the WAKF method. In the NLOS scenario, the maximum error of the traditional KF method is 0.31m, and the average error is 0.27m; the maximum error of the WAKF method is 0.19m, and the average error is 0.17m. Fig 7 and Fig 8 show that the fusion of UWB data and odometry data can eliminate accumulated errors to a certain extent, and the use of WAKF can effectively improve the positioning error problem in NLOS scenarios, and improve positioning accuracy and robustness.

TABLE III
FUSION POSITIONING MEASUREMENT DATA

Point	KF	WAKF	Real	KF Error	WAKF Error
e	(1.55,0.21)	(1.61,0.14)	(1.70,0.00)	0.26	0.17
b	(2.91,-0.16)	(2.93,-0.19)	(3.00,0.00)	0.18	0.20
c	(2.88,-2.08)	(2.92,-2.09)	(3.00,-2.00)	0.14	0.12
f	(2.17,-2.15)	(1.85,-2.12)	(2.00,-2.00)	0.23	0.19
g	(1.17,-1.74)	(1.07,-1.86)	(1.00-2.00)	0.31	0.16
d	(0.04,-1.84)	(0.06,-1.90)	(0.00,-2.00)	0.16	0.12
a	(0.15,-0.08)	(0.07,-0.11)	(0.00,0.00)	0.17	0.13

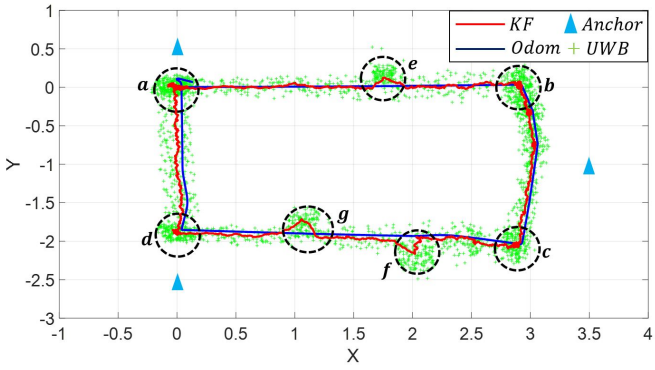

Fig. 7. KF fusion positioning

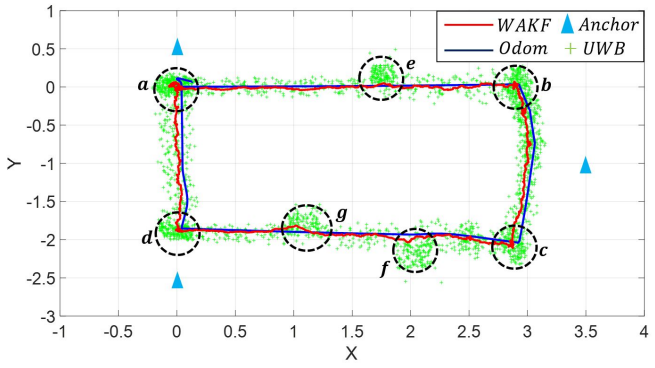

Fig. 8. WAKF fusion positioning

V. CONCLUSIONS

In order to achieve high-precision, low-cost, low-power, and robust positioning of robots in indoor scenarios. Combining the advantages of UWB positioning and odometry position measurement, this paper proposes a method for judging indoor NLOS scenes, and at the same time fuses UWB and odometry by using WAKF algorithm. The experimental results show that the method meets the needs of indoor positioning, and to a certain extent eliminates the cumulative error of the odometry and the influence of the indoor NLOS scene on the positioning of the robot. Its positioning error in the mixed LOS and LOS scenarios is 0.16m, which improves the positioning accuracy and robustness of the robot in indoor environments.

Due to limited testing conditions, there are still many uncertainties in indoor scenarios, which is a huge challenge for the localization of mobile robots. In the future, we will explore UWB anchors deployment, odometry model optimization, fusion algorithm improvement, etc, and establish more test scenarios in different indoor environments to further improve the accuracy and robustness of indoor positioning of mobile robots.

REFERENCES

[1] D. Yu and C. Li, "An Accurate WiFi Indoor Positioning Algorithm for Complex Pedestrian Environments," *IEEE Sensors Journal*, vol. 21, pp. 24440-24452, 2021.

[2] H. Yao, H. Shu, X. Liang, H. Yan and H. Sun, "Integrity Monitoring for Bluetooth Low Energy Beacons RSSI Based Indoor Positioning," *IEEE Access*, vol. 8, pp. 215173-215191, 2020.

[3] A. A. Nazari Shirehjini and S. Shirmohammadi, "Improving Accuracy and Robustness in HF-RFID-Based Indoor Positioning With Kalman Filtering and Tukey Smoothing," *IEEE Transactions on Instrumentation and Measurement*, vol. 69, pp. 9190-9202, 2020.

[4] V. Thio, J. Aparicio, K. Bergh nonsen and J. K. Bekkeng, "Experimental Evaluation of the Forkbeard Ultrasonic Indoor Positioning System," *IEEE Transactions on Instrumentation and Measurement*, vol. 71, pp. 1-13, 2022.

[5] E. Bernardes, S. Viollet and T. Raharijaona, "A Three-Photo-Detector Optical Sensor Accurately Localizes a Mobile Robot Indoors by Using Two Infrared Light-Emitting Diodes," *IEEE Access*, vol. 8, pp. 87490-87503, 2020.

[6] H. Zhang, L. Jin and C. Ye, "An RGB-D Camera Based Visual Positioning System for Assistive Navigation by a Robotic Navigation Aid," *IEEE/CAA Journal of Automatica Sinica*, vol. 8, pp. 1389-1400, 2021.

[7] M. J. Gallant and J. A. Marshall, "Two-Dimensional Axis Mapping Using LiDAR," *IEEE Transactions on Robotics*, vol. 32, pp. 150-160, 2016.

[8] K. Zhao, M. Zhu, B. Xiao, X. Yang, C. Gong and J. Wu, "Joint RFID and UWB Technologies in Intelligent Warehousing Management System," *IEEE Internet of Things Journal*, vol. 7, pp. 11640-11655, 2020.

[9] K. Wen, K. Yu, Y. Li, S. Zhang and W. Zhang, "A New Quaternion Kalman Filter Based Foot-Mounted IMU and UWB Tightly-Coupled Method for Indoor Pedestrian Navigation," *IEEE Transactions on Vehicular Technology*, vol. 69, pp. 4340-4352, 2020.

[10] X. Zhou, H. Zhang, X. Tan and J. Zhang, "A location method based on UWB for ward scene application," *2021 36th Youth Academic Annual Conference of Chinese Association of Automation (YAC)*, pp. 66-71, 2021.

[11] Y. Zheng, Q. Zeng, C. Lv, H. Yu and B. Ou, "Mobile Robot Integrated Navigation Algorithm Based on Template Matching VO/IMU/UWB," *IEEE Sensors Journal*, vol. 21, pp. 27957-27966, 2021.

[12] Y. -Y. Chen, S. -P. Huang, T. -W. Wu, W. -T. Tsai, C. -Y. Liou and S. -G. Mao, "UWB System for Indoor Positioning and Tracking With Arbitrary Target Orientation, Optimal Anchor Location, and Adaptive NLOS Mitigation," *IEEE Transactions on Vehicular Technology*, vol. 69, pp. 9304-9314, 2020.

[13] K. Liu and Z. Li, "Adaptive Kalman Filtering for UWB Positioning in Following Luggage," *2019 34rd Youth Academic Annual Conference of Chinese Association of Automation (YAC)*, pp. 574-578, 2019.

[14] S. Zhang, X. Tan and Q. Wu, "Self-Positioning for Mobile Robot Indoor Navigation Based on Wheel Odometry, Inertia Measurement Unit and Ultra Wideband," *2021 5th International Conference on Vision, Image and Signal Processing (ICVISP)*, pp. 105-110, 2021.

[15] J. Luo, Z. Lin, Y. Li and C. Yang, "A Teleoperation Framework for Mobile Robots Based on Shared Control," *IEEE Robotics and Automation Letters*, vol. 5, pp. 377-384, 2020.

[16] X. Zhu, J. Yi, J. Cheng and L. He, "Adapted Error Map Based Mobile Robot UWB Indoor Positioning," *IEEE Transactions on Instrumentation and Measurement*, vol. 69, pp. 6336-6350, 2020.

[17] J. H. Cheng, P. P. Yu and Y. R. Huang, "Application of Improved Kalman Filter in Under-Ground Positioning System of Coal Mine," *IEEE Transactions on Applied Superconductivity*, vol. 31, pp. 1-4, 2021.